

# Impact of the water symmetry factor on humidification and cooling strategies for PEM fuel cell stacks

D. Picot <sup>\*</sup>, R. Metkemeijer, J.J. Beziau, L. Rouveyre

*Centre d'Energétique, Ecole des Mines de Paris, BP 207, rue Claude Daunesse, F-06904 Sophia Antipolis Cedex, France*

Received 16 February 1998; revised 1 June 1998

---

## Abstract

In this paper, experimental water and thermal balances with three proton exchange membrane fuel cells (PEMFC) are proposed. On the test facility of Ecole des Mines de Paris, three De Nora SPA fuel cell stacks have been successfully studied: An 1 kW<sub>e</sub> prototype using Nafion<sup>®</sup> 117, a 5 and a 10 kW<sub>e</sub> module using Nafion<sup>®</sup> 115. The averaged water symmetry factor determines strategies to avoid drying membrane. So, we propose analytical solutions to find compromises between humidification and cooling conditions, which determines outlet temperatures of gases. For transport applications, the space occupied by the power module must be reduced. One of the main efforts consists in decreasing the operative pressure. Thus, if adequate cooling power is applied, we show experimentally and theoretically the possibility to use De Nora PEM fuel cells with low pressure, without specific external humidification. © 1998 Published by Elsevier Science S.A. All rights reserved.

*Keywords:* Polymer electrolyte fuel cells; Transport applications; Water management; Drying temperature

---

## 1. Introduction

During these last 10 years, several efforts have been made for the integration of proton exchange membrane fuel cells on terrestrial applications such as local power generation and transportation. At the Ecole des Mines de Paris, three industrial De Nora stacks have been successively tested: 1, 5 and 10 kW<sub>e</sub>. A simplified scheme of these stacks is proposed in Fig. 1.

Water and thermal management on these electrochemical reactors are of great importance to satisfy nominal electrochemical efficiency. To maintain a high electrolyte protonic conductivity, a maximal and constant hydration must be made. So, in the De Nora technology, gases (air and hydrogen) are saturated with water vapour at a temperature higher than the operative temperature of cells. In the frame of the European Fuel cell Electrical Vehicle for Efficiency and Range (FEVER) project, we have studied the effect of water and thermal management on these three PEM fuel cells as a function of realistic conditions present in the power module.

## 2. The produced water symmetry factor

In a PEM fuel cell, the fuel and the oxidant compartment are separated by an Electrode Membrane Assembly (EMA). Oxygen from air diffuses into the cathode, where it is electrochemically reduced to water. The same for hydrogen, which diffuses into the anodic electrodes to be oxidized to hydronium ions, which migrate through the membrane to the cathode. The water distribution in the membrane is determined by two main mechanisms: electro-osmotic drag of water by protons transported from anode to cathode and diffusion down the concentration gradient that builds-up [1]. Different mathematical models have been developed in the past to determine water management [2–5]. We introduce in this section the ‘produced

---

<sup>\*</sup> Corresponding author: Tel.: +33-4-93-95-74-10; Fax: +33-4-93-95-75-35; E-mail: picot@cenerg.cma.fr

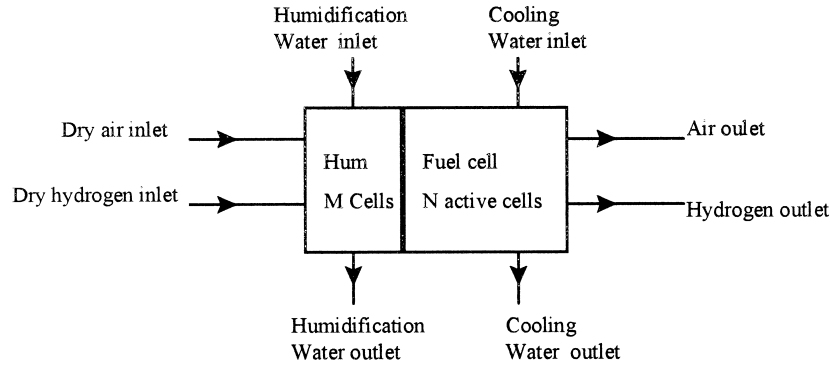


Fig. 1. Simplified De Nora stack architecture.

water symmetry coefficient' which represents the quantity of water produced at the cathode by electrochemical reaction, which is evacuated in the anodic compartment:

$$\alpha = \frac{\text{Water produced evacuated in the anodic compartment}}{\text{Total water produced by the electrochemical reaction}}$$

We cannot access directly to the value of this coefficient. So, the experimental measurements consist of stabilizing the fuel cell with constant global parameters (pressure, flow rates, temperature, current density) and to measure the water production on both anodic and cathodic side. On these fuel cells, we have observed that the evolution of air outlet temperature was an indicator of the fuel cell behaviour. In the literature, a general assumption is to consider each cell as isothermal and the cell temperature is often assumed to be constant. So, in a simplified approach, we consider that the fuel cell temperature corresponds to the temperature of the exhaust air fuel cell stream.

For technological reasons, upstream of the fuel cell, temperatures of gases are inaccessible. Nevertheless, we have developed and validated, with experimental De Nora tests, a numerical model of the humidification system of each module [6]. With standard operative conditions, the relative humidity of gases after humidification can be attributed to 80% (RH = 0.8). To estimate  $\alpha$ , we suggest two water balance estimations: water balance in the anodic and in the cathodic compartment. A description of the experimental system is proposed in Fig. 2.

At the fuel cell outlet, gases are saturated with water (RH = 1). The electrochemically produced water flow rate is given by the faraday law:

$$F_{\text{prod}} = \frac{N \cdot I}{2 \cdot F} \tag{1}$$

with  $I$  the cell current,  $F$  the Faraday's constant and  $N$  the number of cells.

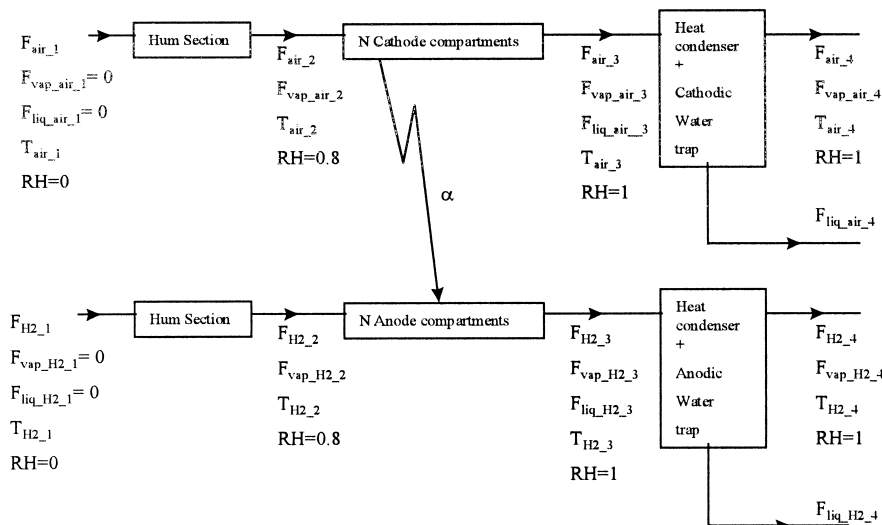


Fig. 2. Experimental presentation of the system.

Table 1  
De Nora PEM fuel cell stacks characteristics and nominal operative conditions

	1 kW <sub>e</sub>	5 kW <sub>e</sub>	10 kW <sub>e</sub>
Nafion® membrane	117	115	115
Membrane thickness (μm)	175	125	125
Cell area (cm <sup>2</sup> ) A	225	900	900
Cells number N	20	21	45
Nominal intensity (A) @ 0.7 V	150	333	333
Total air pressure (bars) P <sub>air</sub>	4	4	4
Total H <sub>2</sub> pressure (bars) P <sub>H2</sub>	3.5	3.5	3.5
Air stoichiometric ratio	2.5	2	2
H <sub>2</sub> stoichiometric ratio	1.5	1.2	1.2

For ideal gas mixtures, the water vapour flow rate for given pressure, temperature and fixed relative humidity is obtained by the following equation:

$$F_{\text{vap}_k}_i = F_{k_i} \cdot \frac{\text{RH} \cdot P_{\text{sat}}(T_{k_i})}{P_k - \text{RH} \cdot P_{\text{sat}}(T_{k_i})} \quad (2)$$

with  $k = (\text{air}; \text{H}_2)$ ,  $i = (1; 2; 3; 4)$  the section of the water balance system (see Fig. 2), RH the relative humidity,  $P_{\text{sat}}$  the saturated vapour pressure,  $P_k$  the total pressure in the compartment  $k$  and  $F_{k_i}$  the dry  $k$  flow rate at the point  $i$ . In this context RH = 0 for  $i = 1$ , RH = 0.8 for  $i = 2$  at standard operative conditions and RH = 1 for  $i = 3, 4$ . With the water balance in the cathodic part, the water symmetry factor corresponds to:

$$\alpha = 1 - \frac{F_{\text{vap\_air}_4} + F_{\text{liq\_air}_4} - F_{\text{vap\_air}_2}}{F_{\text{prod}}} \quad (3)$$

and in the anodic compartment to:

$$\alpha = \frac{F_{\text{vap\_H2}_4} + F_{\text{liq\_H2}_4} - F_{\text{vap\_H2}_2}}{F_{\text{prod}}} \quad (4)$$

To estimate the error of measured values, we can define the following value which is theoretically equal to unity:

$$\theta = \frac{\sum_{k=\text{air}, \text{H}_2} (F_{\text{vap}_k}_4 + F_{\text{liq}_k}_4 - F_{\text{vap}_k}_2)}{F_{\text{prod}}} \quad (5)$$

### 3. Experimental results and discussion

For each De Nora PEM fuel cell stack, we have quantified the water symmetry factor at the test facility of Ecole des Mines de Paris. The main characteristics of these fuel cells are summarized in Table 1.

For the 1 kW<sub>e</sub> fuel cell, the used membrane is the Nafion® 117. For all tested conditions,  $\alpha$  is equal to zero. All water produced is evacuated in the cathodic compartment.

The thickness of Nafion® 115 is lower than Nafion® 117. In Tables 2 and 3, we report 9 tests realized respectively at 30 and 250 A with the 5 kW<sub>e</sub> module, which uses Nafion® 115. In fact, this stack corresponds to a prototype of the 10 kW<sub>e</sub> and the only difference is the cell number. For all tested conditions, we have obtained the same water symmetry factors for the 5

Table 2  
Tests characteristics for the 5 kW<sub>e</sub> PEM fuel cell under 30 A

Case no.	Test time (h)	P <sub>air</sub> / P <sub>H2</sub> (bar/bar)	F <sub>air</sub> (nm <sup>3</sup> /h)	F <sub>H2</sub> (nm <sup>3</sup> /h)	T <sub>air_2</sub> = T <sub>H2_2</sub> (°C)	T <sub>air_4</sub> (°C)	T <sub>H2_4</sub> (°C)
1	4	4.0/3.6	10	3.83	50	47	44
2	1	4.0/3.7	7.88	3.78	27	31	28
3	3	4.0/3.7	12.8	4.05	30	40	35

Table 3  
Tests characteristics for the 5 kW<sub>e</sub> PEM fuel cell under 250 A

Case no.	Test time (h)	$P_{\text{air}}/P_{\text{H}_2}$ (bar/bar)	$F_{\text{air}}$ (nm <sup>3</sup> /h)	$F_{\text{H}_2}$ (nm <sup>3</sup> /h)	$T_{\text{air}_2}$ (°C)	$T_{\text{air}_4}$ (°C)	$T_{\text{H}_2_4}$ (°C)
4	2	4.0/3.7	15.8	3.82	50	57.5	48
5	2	4.0/3.7	7.98	4.1	50.5	61.5	51.5
6	2	4.0/3.7	12.9	4.05	42	57	43.5
7	2	4.0/3.7	12.9	4.05	45	60	46
8	1 h 30 min	4.0/3.6	7.87	3.77	51	63.5	50.5
9	1 h 30 min	4.0/3.6	7.89	3.76	52.5	64	51

and 10 kW<sub>e</sub> stacks. Thus, we present in this part only results for the 5 kW<sub>e</sub> module. For each case, all global parameters are constant and the electric power of the stack is stable. The inlet stack temperatures  $T_{\text{air}_1}$  and  $T_{\text{H}_2_1}$  are considered to be the ambient temperature (20°C).

In Fig. 3, the water symmetry factor varies at 30 A between 10 and 20% without specific humidification (case 2 and 3). Nevertheless when the inlet temperature of gases after humidification is close to outlet values (around 50°C for case 1), between 30 and 35% of produced water is evacuated in the anodic compartment.

In Fig. 4, at 250 A (0.27 A/cm<sup>2</sup>), the water symmetry factor is comprised in a range between 30 and 45%. For all tested global parameters, only the gas temperatures upstream of the fuel cell have an impact on the water distribution.

The experimental error on the water balance is lower to 10% for each case (Fig. 5).

With the present humidification strategy proposed by De Nora, in the frame of the FEVER project, energetic limitations do not permit to obtain gas temperatures higher than 55°C. So, in this case, we conclude that a water symmetry factor of 40% is representative for the water distribution in De Nora PEM fuel cells using Nafion® 115.

On this module, the pressure gradient across the electrolyte is limited by the mechanical structure to an upper value of 0.5 bar. However, the inversion of absolute pressures ( $P_{\text{air}}/P_{\text{H}_2} = 2.5 \text{ bar}/3 \text{ bar}$ ) have no influence on the water symmetry factor. Thus, with this maximum pressure difference of 0.5 bar, water concentrations across electrolyte cannot be represented by hydrodynamic forces [7]. This argument is valid, because the maximum current density for De Nora stacks is 0.33 A/cm<sup>2</sup>. In these conditions, the electro-osmotic forces associated to the passage of current are prevalent on the hydrodynamics forces that depends exclusively on pressure gradients. For inlet air flow rates, a stoichiometric ratio of 2.5 is suggested as performed in the initial FEVER specifications. For the hydrogen loop, an ‘open end’ mode is preferred to ‘dead end’ mode or ‘recirculator’ mode for testing purposes. However, for realistic operations, where there is no need for hydrogen excess, the ‘dead end’ and ‘recirculator’ modes are preferred. In ‘open end’ mode, the hydrogen fuel cell outlet is opened (SFA = 1.2). In ‘dead end’ mode, this outlet is closed by means of an electrovalve (SFA = 1). In the ‘recirculator’ mode, the hydrogen outlet and inlet of the fuel cell are connected via a recirculator. In fact, with air as oxidant, the nitrogen migrates across electrolyte and is accumulated in the anodic compartment for the last two modes. The nitrogen accumulation in the anodic compartment determines the minimum stoichiometric ratio obtainable for hydrogen and was evaluated in our laboratory at 1.03 for ‘dead end’ mode and at 1.00 for recirculator mode [8].

#### 4. Water distribution effects on drying of membrane

If the water symmetry factor is equal to zero, hydrogen must be humidified to avoid water depletion at the anode/membrane interface. Furthermore, if a non-negligible amount of water produced is drained in the anodic

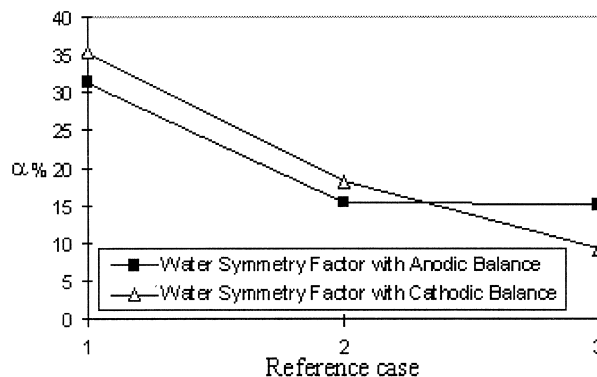


Fig. 3. Produced water symmetry factor for 3 series at 30 A for the 5 kW<sub>e</sub> De Nora Stack.

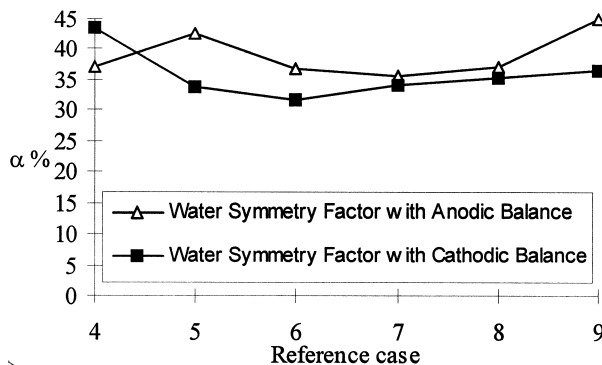


Fig. 4. Produced water symmetry factor for the 5 kW<sub>e</sub> De Nora stack under 250 A.

compartment, drying at the cathode could appear. So, we propose in this part a theoretical analysis to determine thermal balancing and cooling strategies in order to maintain a high fuel cell efficiency.

For each compartment, a criteria to avoid drying can be translated by the following inequalities:

$$F_{\text{vap\_air\_3}} + F_{\text{vap\_air\_2}} < (1 - \alpha) \cdot F_{\text{prod}} \quad (6)$$

for the air side and:

$$F_{\text{vap\_H2\_3}} + F_{\text{vap\_H2\_2}} < \alpha \cdot F_{\text{prod}} \quad (7)$$

for the hydrogen side.

For the saturated vapour pressure, we use a tabulated expression as a function of the temperature which is valid between 20 and 100°C.

$$P_{\text{vap}}(T) = 0.017 \cdot \exp(0.0408 \cdot T) \quad (8)$$

with  $P_{\text{vap}}$  in atm and  $T$  the temperature in °C

Upstream the fuel cell, air and hydrogen flow rates are given respectively by the Faraday laws Eqs. (9) and (10):

$$F_{\text{air\_2}} = \text{SFC} \cdot \frac{N \cdot I}{4 \cdot F} \cdot \frac{1}{x_{\text{O}_2}^0} \quad (9)$$

with SFC the oxygen stoichiometric ratio and  $x_{\text{O}_2}^0$  the inlet oxygen molar fraction.

$$F_{\text{H}_2\_2} = \text{SFA} \cdot \frac{N \cdot I}{2 \cdot F} \quad (10)$$

with SFA the hydrogen stoichiometric ratio.

Downstream of the fuel cell, the respective flow rates are deduced with the stoichiometric consumption Eqs. (11) and (12):

$$F_{\text{air\_3}} = F_{\text{air\_2}} - \frac{N \cdot I}{4 \cdot F} \quad (11)$$

for air and

$$F_{\text{H}_2\_3} = F_{\text{H}_2\_2} - \frac{N \cdot I}{2 \cdot F} \quad (12)$$

for hydrogen.

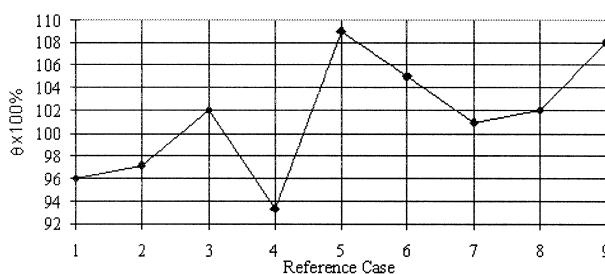


Fig. 5. Estimation of the error on measured water produced for each case.

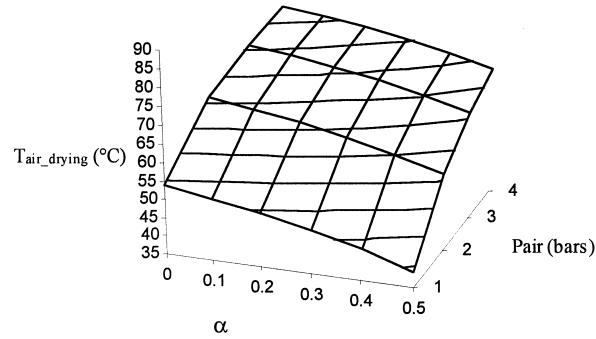


Fig. 6. Limiting air exhaust temperature as a function of water symmetry factor and total pressure without humidification.

Introducing the expressions Eqs. (1), (2), (8), (9) and (11) in Eq. (6) and Eqs. (1), (2), (8), (10) and (12) in Eq. (7), we can extract the critical exhaust gas stream temperature for air and hydrogen to avoid drying:

$$T_{\text{air\_drying}} = \frac{1}{0.0408} \cdot \ln \left\{ \frac{P_{\text{air}}}{0.017} \cdot \frac{\text{SFC} \cdot \frac{\text{RH} \cdot P_{\text{vap}}(T_{\text{air}_2})}{P_{\text{air}} - \text{RH} \cdot P_{\text{sat}}(T_{\text{air}_2})} + 2 \cdot x_{\text{O}_2}^0 \cdot (1 - \alpha)}{\text{SFC} - x_{\text{O}_2}^0 + 2 \cdot x_{\text{O}_2}^0 \cdot (1 - \alpha) + \text{SFC} \cdot \frac{\text{RH} \cdot P_{\text{vap}}(T_{\text{air}_2})}{P_{\text{air}} - \text{RH} \cdot P_{\text{vap}}(T_{\text{air}_2})}} \right\} \quad (13)$$

$$T_{\text{H}_2\_drying} = \frac{1}{0.0408} \cdot \ln \left\{ \frac{P_{\text{H}_2}}{0.017} \cdot \frac{\text{SFC} \cdot \frac{\text{RH} \cdot P_{\text{vap}}(T_{\text{H}_2_2})}{P_{\text{H}_2} - \text{RH} \cdot P_{\text{vap}}(T_{\text{H}_2_2})} + \alpha}{\text{SFA} - 1 + \alpha + \text{SFA} \cdot \frac{\text{RH} \cdot P_{\text{vap}}(T_{\text{H}_2_2})}{P_{\text{H}_2} - \text{RH} \cdot P_{\text{vap}}(T_{\text{H}_2_2})}} \right\} \quad (14)$$

These two analytical expressions are independent on the current and number of cells.

In Figs. 6 and 7 we report the limiting air exhaust temperature respectively for dry and saturated air at the inlet fuel cell as a function of the water symmetry factor and of the absolute pressure at fixed stoichiometry.

Without humidification, for an absolute air pressure of 4 bar, membrane drying occurs with temperatures higher than 72°C for  $\alpha = 0.5$  and 95°C for  $\alpha = 0$ . For transport applications, the use of low pressure is essential to reduce the power consumed by the compressor system. When the air pressure decreases, the water vapour in gases increases and the cooling system must be able to satisfy lower air outlet temperatures. Thus, without humidification, with a symmetry factor equal to 0.4 and  $P_{\text{air}} = 1.5$  bar,  $T_{\text{air}_3}$  must be lower than 40°C.

In the case where saturated air is used ( $\text{RH} = 1$ ), and where the water symmetry factor is lower than 0.5, drying problems are avoided if the difference between outlet and inlet air temperature is smaller than 15°C (for pressures higher than 2 bar and  $\alpha < 0.6$ ).

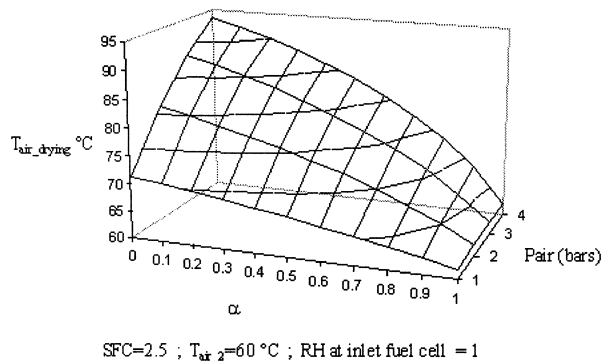


Fig. 7. Limiting air exhaust temperature as a function of water symmetry factor and total pressure with air saturated upstream of the fuel cell.

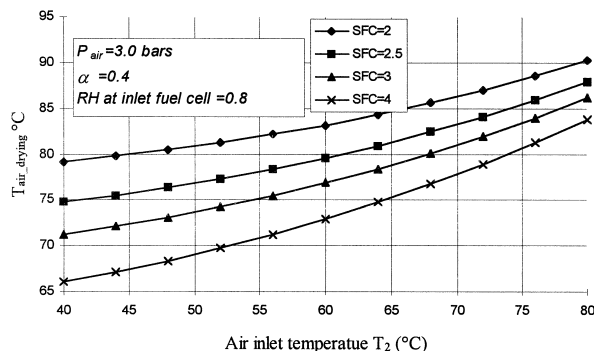


Fig. 8. Limiting air exhaust temperature for 5 and 10 kW<sub>e</sub> De Nora fuel cells as a function of air temperature upstream of the fuel cell.

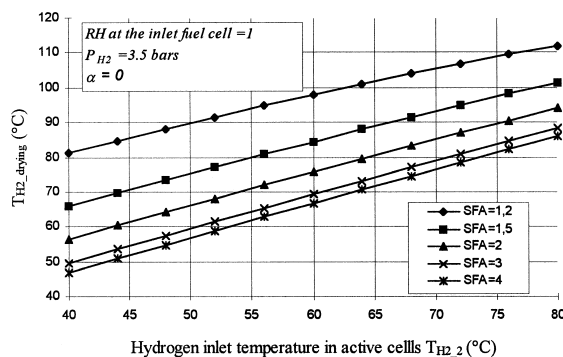


Fig. 9. Limiting hydrogen exhaust temperature for the 1 kW<sub>e</sub> De Nora fuel cell for different stoichiometric ratios.

With De Nora fuel cell stacks, the outlet temperature is determined by the cooling system. In the frame of the FEVER project, an air pressure of 3 bar is used. So in Fig. 8, we propose limiting air exhaust temperature as a function of the inlet air temperature at various stoichiometric coefficients for a 5 and a 10 kW<sub>e</sub> module.

In dynamic regime with urban cycle, we will meet idling conditions. Under these conditions, due to compressor strategies, stoichiometric ratios can go up to values as high as 5. With a maximal air inlet temperature of 55°C, problems can occur with exit air temperatures higher than 70°C. This limit of operation has been observed during experimental tests.

For the 1 kW<sub>e</sub> De Nora PEM fuel cell stack,  $\alpha$  is equal to zero and the drying problem can occur in anodic section. The same analysis is proposed in Fig. 9.

In this configuration, it is preferred to introduce saturated hydrogen at a temperature higher than the ‘operating value’. Furthermore, with the electro-osmotic effect, a humidified anode/membrane interface must be maintained.

## 5. Impact on cooling system

The foregoing analysis gives conditions for temperatures and relative humidities between upstream and downstream fuel cell to avoid drying problems. If upstream conditions for gases depend on system humidification, the cooling loop fixes the outlet cell temperature.

Table 4  
Constant parameters of Eq. (16) for the 10 kW<sub>e</sub> De Nora Fuel Cell

10 kW <sub>e</sub> De Nora PEM fuel cell	
$a_0$	17.9302 V
$a_1$	0.0212 V/K
$a_2$	0.00705 V/K
$a_3$	−0.008844 V/K
$a_4$	−0.24734 V/K
$a_5$	−0.010605 Ω

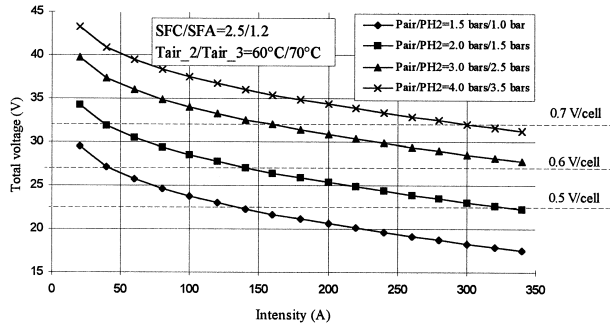


Fig. 10.  $U/I$  curves of the 10 kW<sub>e</sub> De Nora stack for different total pressures and temperatures.

Heat dissipation by electrochemical reaction is a function of the electric response and can be expressed by the following relation:

$$Q_{\text{stack}} = N \cdot I \cdot E_{\text{thn}} - N \cdot I \cdot U_{\text{stack}} \tag{15}$$

where  $Q_{\text{stack}}$  represents the heating power expressed in watts,  $E_{\text{thn}}$  is the thermoneutral cell voltage which is 1.48 V ( $\Delta H/nF$ ) and not 1.23 V, the thermodynamic voltage.  $U_{\text{stack}}$  corresponds to the total voltage of the fuel cell.

With a global energetic balance between inlet and outlet of the fuel cells, an empirical expression of the total voltage must be proposed for each studied fuel cell.

For this reason, we use an expression for 10 kW<sub>e</sub> De Nora stacks which do not have a theoretical validity but realistically characterizes its electric behaviour as a function of global parameters [9]:

$$U_{\text{stack}} = a_0 + a_1 \cdot T_{\text{air}_3} \cdot \ln(P_{\text{H2mean}}) + a_2 \cdot T_{\text{air}_3} \cdot \ln(P_{\text{O2mean}}) + a_3 \cdot T_{\text{air}_3} \cdot \ln(I) + a_4 \cdot T_{\text{air}_3} + a_5 \cdot (I) \tag{16}$$

where  $T_{\text{air}_3}$  is the exhaust air temperature in K,  $P_{\text{H2mean}}$  and  $P_{\text{O2mean}}$  respectively the hydrogen and oxygen mean partial pressure between inlet and outlet fuel cells expressed in Pa. The constants  $a_i$  have been determined by various tests and are summarized in the Table 4 for the 10 kW<sub>e</sub> stack.

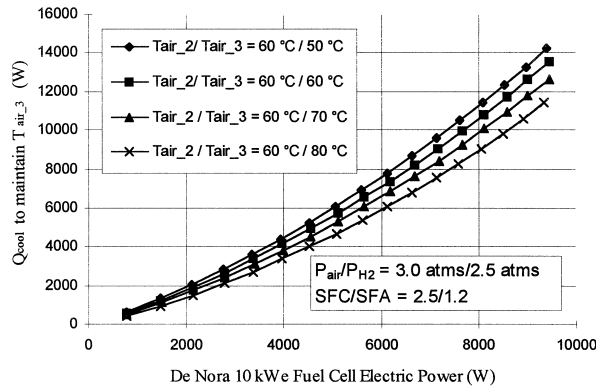


Fig. 11. Necessary cooling power for the De Nora 10 kW<sub>e</sub> PEM fuel cell as a function of electric power for different outlet air temperatures.

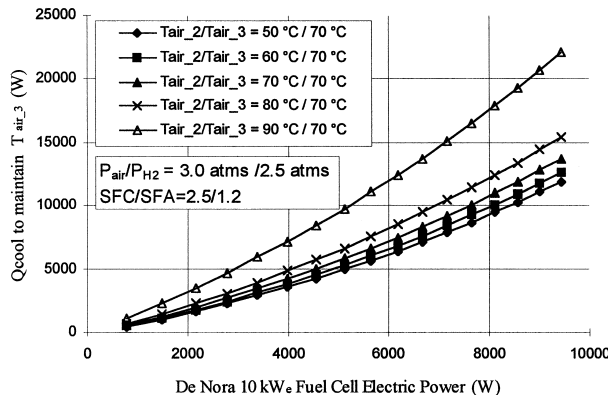


Fig. 12. Necessary cooling power for the De Nora 10 kW<sub>e</sub> PEM fuel cell as a function of electric power for different inlet air temperatures.



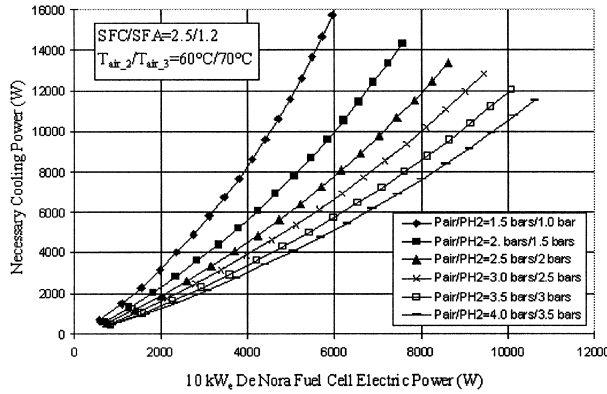


Fig. 13. Necessary cooling power for the De Nora 10 kW<sub>e</sub> PEM fuel cell as a function of electric power for different absolute pressures.

The various absolute pressure, voltage/current responses of the 10 kW<sub>e</sub> are plotted in Fig. 10: The total thermal power of the gases flowing into the fuel cell is expressed by:

$$E_{in} = \sum_{k=(air;H_2;H_2O_{vap})} F_{k_{-2}} \cdot C_{p_{-k}} \cdot (T_{k_{-2}} - T_{ref}) \quad (17)$$

with  $C_{p_{-k}}$  the molar heat capacity in J/mole/K and  $T_{ref}$  the reference temperature (20°C).

For the exhaust gases, a similar relation is proposed:

$$E_{out} = \sum_{k=(air;H_2;H_2O_{vap};H_2O_{liq})} F_{k_{-3}} \cdot C_{p_{-k}} \cdot (T_{k_{-3}} - T_{ref}). \quad (18)$$

In the total energetic balance we take into account the latent heat of evaporation or condensation. Thus, the cooling power, which is necessary to maintain outlet temperature, corresponds to:

$$Q_{cool} = E_{in} - E_{out} + Q_{stack} + L_{vap} \cdot \sum_{k=(air;H_2)} (F_{vap_{k-2}} - F_{vap_{k-3}}) \quad (19)$$

with  $L_{vap}$  the evaporation heat latent in J/mole.

For given exhaust gas temperatures, the cooling power is obtained by introducing relations Eqs. (15)–(18) in Eq. (19).

For the following results, we assume that the hydrogen temperature at the inlet and outlet of the fuel cell are identical to air temperature.

In Fig. 11, with inlet saturated gases at 60°C, the necessary cooling power is reported for various exhaust gas temperatures for the 10 kW<sub>e</sub> PEM fuel cell.

In Fig. 12, the necessary cooling power for 10 kW<sub>e</sub> fuel cell stack is plotted as a function of electric power for various inlet gas temperatures. When inlet gas temperature increases and becomes higher than exhaust gas temperatures, the water condensation in the fuel cell is translated in an overheating of the system. So, an additional cooling power is necessary to maintain outlet temperature (70°C in this example).

In Fig. 13, various cooling powers are compared for several absolute pressures. With realistic heat and flow rate conditions, we show the feasibility to use De Nora fuel cell with low pressure. With the standard power cooling in the 10 kW<sub>e</sub> fuel cell (11 kW), we can obtain about 5 kW<sub>e</sub> at 1.5 bar for air. If the cooling power is increased to 16 kW at the same pressure, the maximum electric power is equal to 6 kW<sub>e</sub> (60% of the total electric power).

## 6. Conclusions

Water and thermal management in PEM fuel cell stacks are fundamental. Even if several authors in literature report mathematical models on this subject [2–5], the numerical calculation of produced water symmetry factor is ambiguous to be determined with membranes different from Nafion<sup>®</sup> 117. On the fuel cell test facility at the Ecole des Mines de Paris, we have made water and thermal balances with 1, 5 and 10 kW<sub>e</sub> De Nora PEM fuel cell stacks. With Nafion<sup>®</sup> 117, we have found that all water produced was evacuated in the cathodic part. By using Nafion<sup>®</sup> 115, our analysis shows an average water symmetry factor equal to 40% for all global parameters in a range of current density lower than 0.4 A/cm<sup>2</sup>. With a simplified system energetic approach, we derive the operative temperatures to avoid membrane drying. The water symmetry

effect on humidification and cooling applications shows the use of strategies for a given application. In laboratory conditions, it is possible to use a fuel cell without humidification if cooling power is increased to compensate the overheating released by the electrochemical reaction. For transport applications, where the cooling power is limited by available space in the module, gas humidification upstream of the fuel cell is primordial.

## 7. List of symbols

$A$	fuel cell surface, $\text{cm}^2$
$C_{p,i}$	molar heat capacity of specie $i$ , $\text{J/mole/K}$
$E_{\text{in}}$	inlet gases fuel cell heating power, $\text{W}$
$E_{\text{out}}$	outlet gases fuel cell heating power, $\text{W}$
$E_{\text{thn}}$	cell thermoneutral voltage, $\text{V}$
$F$	Faraday's constant, $F = 96,487 \text{ C/equivalent}$
$F_{\text{air}}$	molar air flow rate, $\text{mole/s}$
$F_{\text{H}_2}$	molar hydrogen flow rate, $\text{mole/s}$
$F_{\text{prod}}$	molar water flow rate produced by electrochemical reaction, $\text{mole/s}$
$I$	cell current, $\text{A}$
$L_{\text{vap}}$	heat of evaporation, $\text{J/mole}$
$N$	number of cells in the stack
$P_{\text{air}}$	total pressure in cathodic compartment, $\text{atm}$
$P_{\text{H}_2}$	total pressure in anodic compartment, $\text{atm}$
$P_{\text{vap}}$	saturated vapour pressure, $\text{atm}$
PEM	Proton Exchange Membrane
$Q_{\text{cool}}$	cooling power, $\text{W}$
$Q_{\text{stack}}$	heat power produced by electrochemical reaction for the stack, $\text{W}$
RH	relative humidity
SFA	hydrogen stoichiometric ratio
SFC	air stoichiometric ratio
$U_{\text{stack}}$	fuel cell voltage, $\text{V}$
$T$	temperature, $^{\circ}\text{C}$
$T_{\text{ref}}$	reference temperature for the system, $^{\circ}\text{C}$
$x_{\text{O}_2}^0$	molar oxygen fraction at the stack inlet.
<i>Greek letters</i>	
$\alpha$	produced water symmetry factor
$\theta$	experimental water balance error

## Acknowledgements

The presented work was carried out as a part of the FEVER project. Co-workers Mr. Patrick Achard and Mr. Patrick Leroux from the energetic center of Ecole des Mines de Paris are acknowledged for valuable discussions and for PEM fuel cells test facilities. Mr. Claudio Mantegazza and Mr. Antonio Maggiore from De Nora are gratefully acknowledged for their attentive collaboration.

## References

- [1] T.A. Zawodzinski Jr., T. Springer, F. Uribe, S. Gottesfeld, *Solid State Ionics* 60 (1993) 199–211.
- [2] D.M. Bernardi, *J. Electrochem. Soc.* 137 (1990) 3344–3350.
- [3] T. Nguyen, R.E. White, *J. Electrochem. Soc.* 140 (1993) 2178–2186.
- [4] D.M. Bernardi, M.W. Verbrugge, *J. Electrochem. Soc.* 139 (1992) 2477–2490.
- [5] T.E. Springer, T.A. Zawodzinski, S. Gottesfeld, *J. Electrochem. Soc.* 138 (1991) 2334–2342.
- [6] D. Picot, Thesis of Ecole des Mines de Paris, 1998.
- [7] L. Gerboux, ENSEEG thesis, 1997.
- [8] R. Metkemeijer, L. Rouveyre, P. Achard, D. Picot, Hypothesis II Conference, Grimstadt, Norway, 1997.
- [9] L. Rouveyre, Thesis of Ecole des Mines de Paris, 1998.